

# APPLICATION OF MICROTREMOR MEASUREMENTS TO THE ESTIMATION OF EARTHQUAKE GROUND MOTIONS IN KUSHIRO CITY DURING THE KUSHIRO-OKI EARTHQUAKE OF 15 JANUARY 1993

TAKEYASU SUZUKI, YOSHITAKA ADACHI AND MINATO TANAKA

*Technical Research and Development Institute, Kumagai Gumi Co., Ltd., 1043 Shimoyama, Onigakubo, Tsukuba-shi, Ibaraki 300-22, Japan*

## SUMMARY

Microtremor measurements were conducted in Kushiro City, Hokkaido Island of Japan. The thickness of alluvial deposits in the central area of Kushiro City abruptly changes from 0 to 80 m. Predominant ground motion at a microtremor measuring site is represented by the spectral ratio, the ratio of Fourier amplitude spectrum of microtremor in the horizontal direction to that in the vertical direction. The peak frequency of the spectral ratio corresponds well to the predominant frequency estimated from the thickness of alluvial layer at each site. Based on a hypothesis that the spectral ratio can be regarded identical with a half of the amplification factor from diluvial bed rock to the ground surface, the strong ground motion due to the Kushiro-oki earthquake at each site is estimated. The method of estimation is verified by the comparison of the synthesized accelerogram with the recorded one at West Port of Kushiro. The results satisfactorily explain major damages and vibrations felt in Kushiro City during the earthquake.

## INTRODUCTION

The Kushiro earthquake of  $M = 7.8$  struck the eastern part of Hokkaido Island in Japan on 15 January 1993. Kushiro City is located only 16 km away from the epicentre (see Figure 1). Kushiro District Meteorological Observatory recorded the maximum acceleration of 922 gals in the horizontal direction. Major seismic damages appeared as landslide in and around Kushiro City, and trunk pipelines for gas and water suffered from damage in the diluvial hill area, and liquefaction was observed in the port and harbour area.<sup>1</sup> Very little destructive damage occurred within the Kushiro Plain. However, subsidence due to the earthquake, measuring over 20 cm, took place in the northern area of Kushiro City, where newly constructed housing developments are distributed.

The central area of Kushiro City extends about  $8 \text{ km} \times 6 \text{ km}$ . Within such a small area, the thickness of alluvial deposits abruptly changes from 0 to 80 m. A diluvial hill is located in the southeastern part of the city. From these geological conditions, the city is regarded as one of the sites most suitable for establishing a method to evaluate seismic risks in relation to the effect of surface geology on seismic motion.

It is well known that microtremors represent predominant vibrations of the surface layer, corresponding to local geological conditions. Microtremor measurements have recently implemented more frequently for the purpose of determining natural periods of local sites. Nakamura<sup>2</sup> and Nakamura and Takizawa<sup>3</sup> applied microtremor technique to the estimation of dynamic characteristics of embankments and the estimation of the thickness of alluvial layers as well as to their shear wave velocity, resorting to a 'spectral ratio' which is defined as the ratio of Fourier amplitude spectrum of microtremor in the horizontal direction to that in the vertical direction. Nakamura *et al.*,<sup>4</sup> and Ohmachi and Nakamura<sup>5</sup> have tried to explain earthquake damages, by assuming the spectral ratio of microtremors measured at damaged sites as amplification factors.

The first approach of this paper is to demonstrate how the spectral ratio of microtremor defined above represents predominant vibration of surface soil deposits. The second is to synthesize earthquake ground

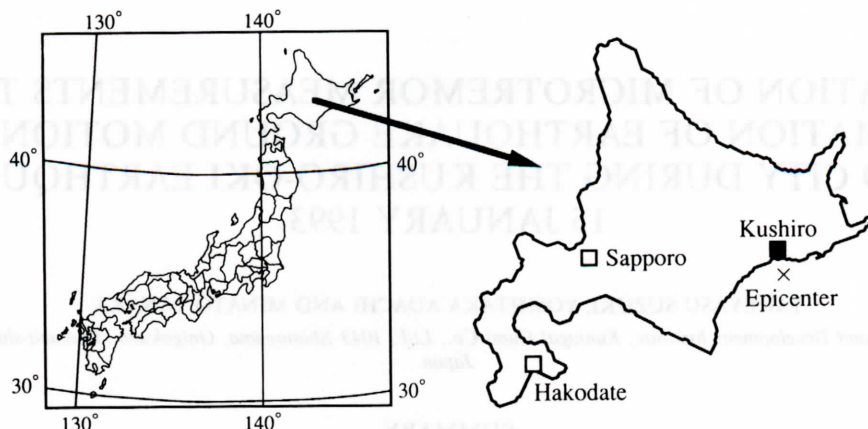


Figure 1. Map of Japan and the location of Kushiro City in Hokkaido Island

motions which are observed during the Kushiro-oki earthquake, on a hypothesis that the earthquake damages Kushiro City suffered may be clearly explained in terms of spectral ratios.

### GROUND CONDITIONS IN KUSHIRO CITY

The surface ground condition of Kushiro City is classified into three categories, that is, old sand dune area, fill over marsh or marsh and diluvial hill. Figure 2 is a map of the central area of Kushiro City, in which zones are classified according to the three geological conditions. As shown in the figure, the old sand dune area extends in the southern part facing the Pacific Ocean. An area of fill over marsh exists in the northern area of the city. East of the Old Kushiro River, a hill of diluvial loam deposit develops at the altitude of 30–40 m, extending from the deposit underlying the alluvial layer in the Kushiro Plain.

Figure 3 is the thickness contour map for alluvial deposits and Figure 4 that of a peat deposit in Kushiro City.<sup>6</sup> The alluvial deposits vary in thickness from 10 to 80 m in the plain. The deepest part of the deposits reaching 80 m is located at the mouth of the Kushiro River. In the area near Katsuragi, the thickness of alluvial deposits changes abruptly and complexly from 70 to 30 m. In the north of the city, there is a peat layer 1–4 m deep, having its maximum thickness at Ashino which, as shown in Figure 4, lies between the Kushiro River and the Old Kushiro River.

The diluvial hill is extremely undulated. In the north of the hill, at Midorigaoka, there are housing developments which were constructed in 1960s by the municipal authorities of Kushiro City. This area was developed, cutting slopes and filling valleys along the previous geometry of the hill. Damages due to the Kushiro earthquake concentrated in this area where large-scale slope failure and severe damage of gas pipelines took place.

### SITES AND METHOD OF MICROTREMOR MEASUREMENTS AND PROCESSING OF MICROTREMOR DATA

Microtremor measurements were implemented in March and May 1993 in Kushiro City in order to compare the result of measurements in winter with that in spring. As Kushiro City is located on the latitude of 40°N, the surface soils 1.0–1.5 m thick is frozen until early May. We can assume that frozen surface soil would largely affect the earthquake ground motions in Kushiro City at the time of the Kushiro-oki earthquake.

Sites of microtremor measurements conducted are marked with black squares in Figure 2. Measurements were carried out at a total of 20 sites. At 16 out of 20 sites, measurement was conducted in the daytime both in March and May, and by using the remaining four sites, additional measurement was conducted in May at the sites for which no data sampling had been made.



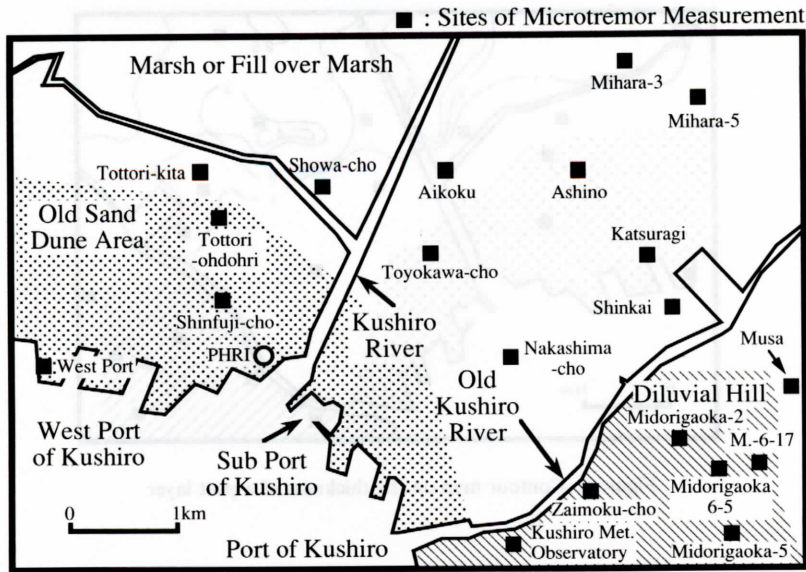


Figure 2. Classification corresponding to ground conditions and microtremor measuring sites in the central area of Kushi City

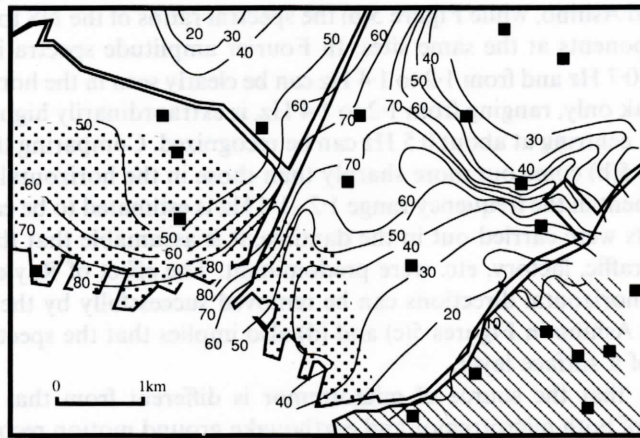


Figure 3. Contour map on the thickness of alluvial deposits

The three components of velocity, in the horizontal north–south (NS), east–west (EW) directions and in the vertical (UD) direction were recorded three times at each site with a high-pass filter of 0.1 Hz. The number of data points sampled is 8192 and the sampling interval is 100 Hz. Fourier amplitude spectra of microtremor data were determined first. Smoothing operation was applied successively three times to every component of the spectrum, using the Hanning window in order to make smoothing more effective. An average spectrum in each direction at each site was determined by averaging three spectra in each direction. Finally, spectral ratios of average Fourier amplitude spectra of the NS and EW components, respectively, to that of the UD component,  $SR_{NS}(\omega)$  and  $SR_{EW}(\omega)$ , are obtained as follows:

$$SR_{NS}(\omega) = \frac{F_{NS}(\omega)}{F_{UD}(\omega)}, \quad SR_{EW}(\omega) = \frac{F_{EW}(\omega)}{F_{UD}(\omega)} \quad (1)$$



Figure 4. Contour map on the thickness of a peat layer

in which  $F_{NS}(\omega)$  is the Fourier amplitude spectrum in the NS direction,  $F_{EW}(\omega)$  the Fourier amplitude spectrum in the EW direction and  $F_{UD}(\omega)$  the Fourier amplitude spectrum in the UD direction.

Figure 5 gives two examples to show that predominant vibration of surface deposits can be grasped by means of spectral ratio. Figure 5(a) shows Fourier amplitude spectra of three components of a microtremor recorded at West Port and Ashino, while Figure 5(b) the spectral ratios of the NS to the UD components and the EW to the UD components at the same sites. In Fourier amplitude spectra in Figure 5(a), two major peaks ranging from 0.5 to 0.7 Hz and from 1.2 to 1.4 Hz can be clearly seen in the horizontal directions, while in the UD direction, one peak only, ranging from 1.2 to 1.4 Hz, is extraordinarily high. In spectral ratios, on the other hand, only the peak centring at about 0.5 Hz can be recognized. Comparing the two figures of the same site, the spectra in Figure 5(b) come out more sharply than those in the horizontal directions in Figure 5(a). The microtremor component in the frequency range 1.2–1.4 Hz is estimated to be caused mainly by Rayleigh wave. Since measurements were carried out in the daytime, it is assumable that the origins of microtremor causing Rayleigh wave, traffic, factory, etc. were predominant. The effect of Rayleigh wave on the Fourier amplitude spectra in the horizontal directions can be removed successfully by the use of the spectral ratio. The comparison made at Ashino in Figures 5(c) and (d) also implies that the spectral ratio clearly gives the predominant frequency of a surface layer.

Lu *et al.*<sup>7</sup> pointed out that the source of microtremor is different from that of an earthquake. They compared power spectra of both microtremor and earthquake ground motion recorded at the same site and concluded that both horizontal and vertical motions in microtremor were originated from a similar source, while horizontal motion is mainly caused by S-wave and vertical motion by both S- and P-wave in an earthquake. Nakamura<sup>8</sup> defined the spectral ratio as the spectral amplification factor, based on a hypothesis that the vertical motion at bed rock is almost identical with that of the horizontal motion. Thus, the authors assume that the amplification factor at ground surface which should work on the wave incidence with unit amplitude at bed rock,  $F_{amp}(\omega)$ , can be approximated by the spectral ratio,  $SR(\omega)$ , in the following relation:

$$F_{amp}(\omega) = 2 SR(\omega) \quad (2)$$

Based on the assumption given above, microtremor data are examined using the spectral ratio. Then, the spectral ratio, being given as a half of the amplification factor, is applied to synthesize the earthquake ground motions at microtremor measuring sites in Kushiro City during the Kushiro-oki earthquake.

### SPECTRAL RATIOS IN KUSHIRO

Spectral ratios for six representative sites out of 20 are given in Figures 6(a) and (b). As shown in the figures, the peak at a predominant frequency of the surface layer can be clearly seen, especially in spectral ratio for



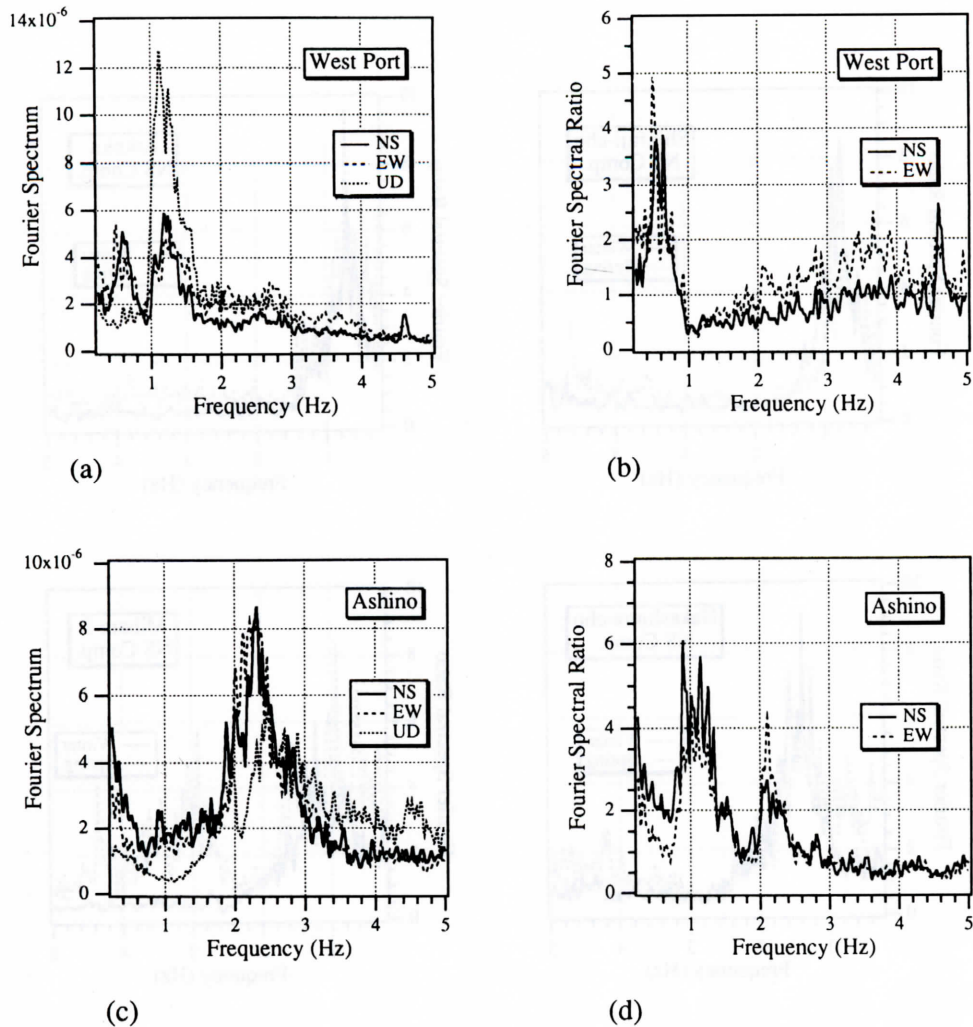


Figure 5. Comparison between Fourier spectra and spectral ratios for microtremor measured in the daytime at West Port and Ashino, (a) Fourier spectra at West Port, (b) Spectral ratios at West Port, (c) Fourier spectra at Ashino, (d) Spectral ratios at Ashino

four sites, Shinfuji-cho, Aikou, Nakashima-cho and Mihara-3 in the Kushiro Plain. The minimum value of the spectral ratio, which exists in the frequency range higher than 2 Hz, is around 1.0, which seems to justify the hypotheses discussed in the previous chapter. Peaks for the second or the third mode of shear vibration do not appear clearly at the four sites. However, it is well known that higher modes are generally weaker in predominance than the fundamental mode in the amplification factor for multiple layered soil deposits.

Comparing Figure 6(a) with Figure 6(b), shapes and peaks of spectral ratios in the NS and the EW directions are known to be almost coincident with each other. Comparing the spectral ratio in winter with that in spring in Figures 6(a) and (b), no conspicuous difference can be seen, except the fact that the values of the ratio at frequency higher than 2.0 Hz are a little larger in spring than in winter. Resorting to the multiple reflection theory, it can be explained why the amplification in higher modes becomes low when soil deposits are covered with thin and hard material. However, it can be concluded that the earthquake ground motion in winter is not so different from that in spring. Thus, such coincidence of spectral ratios measured at different moments implies well the validity of microtremor measurements.

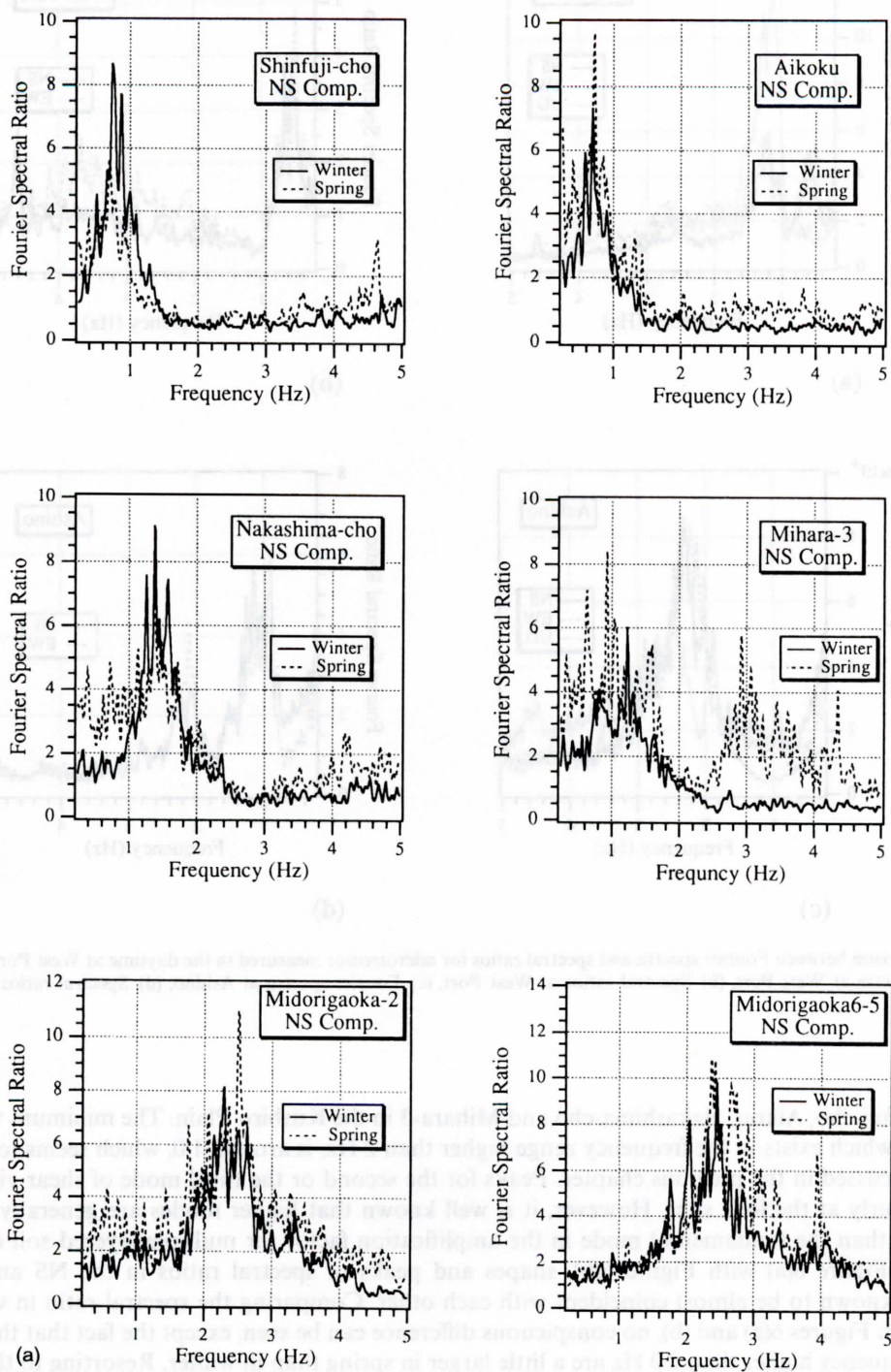


Figure 6(a). NS components of spectral ratio derived from the microtremor data, measured in March (winter) and those measured in May (spring) in Kushiro City



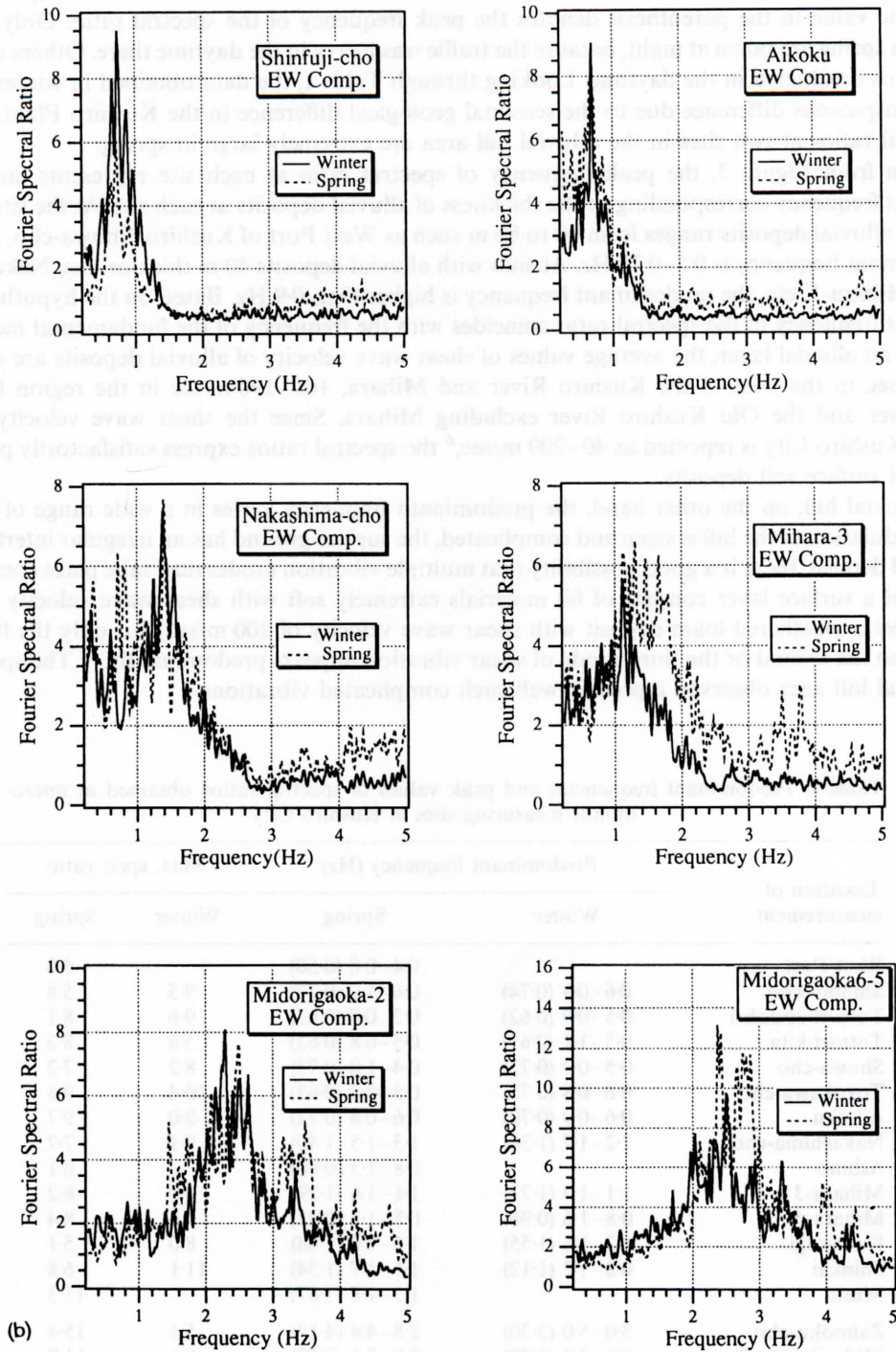


Figure 6(b). EW components of spectral ratio derived from the microtremor data, measured in March (winter) and those measured in May (spring) in Kushiro City

Predominant frequency ranges, peak frequencies and peak spectral ratios observed at microtremor measuring sites are summarized in Table I. In the table, results obtained in both winter and spring are stated together. The value in the parenthesis denotes the peak frequency of the spectral ratio. Only the data at Katsuragi in spring are taken at night, because the traffic was heavy in the daytime there. Others are results of measurements conducted in the daytime. Looking through Table I, the data obtained in winter and spring show no conspicuous difference due to the seasonal geological difference in the Kushiro Plain, though the peak spectral ratios at two sites in the diluvial hill area are extremely large in spring.

As known from Figure 3, the peak frequency of spectral ratio at each site represents fairly well the predominant frequency corresponding to the thickness of alluvial deposits at each site. At the sites where the thickness of alluvial deposits ranges from 40 to 80 m such as West Port of Kushiro, Showa-cho, Aikoku, etc. the predominant frequency is 0.5–0.75 Hz. At sites with alluvial deposits 40 m thick or less, Nakashimo-cho, Mihara-3, Mihara-5, etc. the predominant frequency is higher than 0.9 Hz. Based on the hypothesis that the predominant frequency of the spectral ratio coincides with the frequency of the fundamental mode of shear vibration of an alluvial layer, the average values of shear wave velocity of alluvial deposits are estimated as 110–140 m/sec in the west of the Kushiro River and Mihara, 160–190 m/sec in the region between the Kushiro River and the Old Kushiro River excluding Mihara. Since the shear wave velocity of alluvial deposits of Kushiro City is reported as 40–200 m/sec,<sup>6</sup> the spectral ratios express satisfactorily predominant vibrations of surface soil deposits.

In the diluvial hill, on the other hand, the predominant frequency varies in a wide range of 1.8–4.2 Hz. Since the undulation of the hill is steep and complicated, the surface ground has an irregular interface. In such a surface soil deposit, there is a good possibility that multiple vibration modes may take place combinedly.<sup>9</sup> If the profile of a surface layer consists of fill materials extremely soft with shear wave velocity of 50 m/sec which overlies a weathered loam deposit with shear wave velocity of 200 m/sec, not only the fundamental mode but also the second or the third mode of shear vibration appears predominantly.<sup>10</sup> The spectral ratios of the diluvial hill area observed represent well such complicated vibrations.

Table I. Predominant frequencies and peak values of spectral ratios obtained at microtremor measuring sites in Kushiro City

Location of measurement	Predominant frequency (Hz)		Max. spec. ratio	
	Winter	Spring	Winter	Spring
West Port		0.4–0.8 (0.50)		5.0
Shin-fuji-cho	0.6–0.9 (0.74)	0.6–1.0 (0.72)	9.5	5.8
Tottori-ohdohri	0.5–0.9 (0.62)	0.3–0.7 (0.63)	9.6	8.1
Tottori-kita	0.5–1.1 (0.67)	0.5–0.8 (0.62)	5.8	8.3
Showa-cho	0.5–0.9 (0.72)	0.4–1.0 (0.73)	8.2	7.2
Toyokawa-cho	0.6–0.8 (0.72)	0.5–0.8 (0.63)	10.4	9.8
Aikoku	0.6–0.9 (0.70)	0.6–0.8 (0.72)	9.0	9.7
Nakashima-cho	1.2–1.7 (1.38)	1.3–1.5 (1.40)	9.1	7.7
Ashino		0.8–1.3 (0.90)		6.1
Mihara-3	1.1–1.4 (1.23)	1.1–1.6 (1.29)	6.0	8.2
Mihara-5	0.8–1.6 (0.96)	0.8–1.2 (0.93)	7.6	8.4
Katsuragi	1.3–1.8 (1.55)	1.5–1.8 (1.68)	8.0	5.1
Shinkai	0.8–1.2 (1.12)	1.1–1.7 (1.54)	11.1	6.8
Musa		1.5–1.8 (1.67)		11.3
Zaimoku-cho	3.0–5.0 (3.30)	2.8–4.4 (4.14)	5.1	15.4
Midorikaoka-2	2.0–2.7 (2.29)	2.0–2.6 (2.50)	8.1	11.0
Midorigaoka-6-5	1.9–2.9 (2.50)	2.3–2.9 (2.38)	9.8	13.2
Midorigaoka-6-17	1.5–2.8 (1.81)	1.7–2.0 (1.88)	6.2	24.0
Midorigaoka-5	Not clear	Not clear	4.4	2.6
Meteoro. Observ.		3.9–4.7 (4.31)		10.1



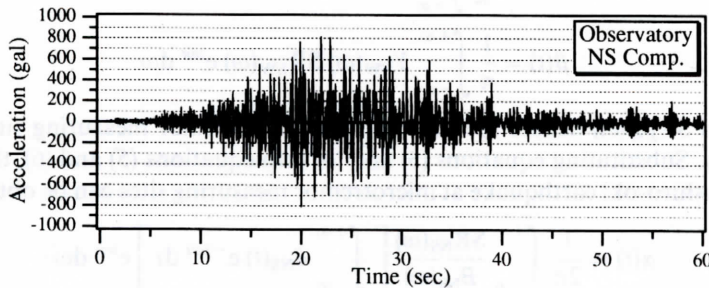
# ESTIMATION OF EARTHQUAKE GROUND MOTIONS IN KUSHIRO DURING THE KUSHIRO-OKI EARTHQUAKE

Kushiro District Meteorological Observatory located on the diluvial hill recorded 922.2 gals and 817.4 gals at maximum in the EW and the NS directions, respectively, during the Kushiro-oki earthquake.<sup>11</sup> The displacement in the NS direction was 11.1 cm at maximum which was twice as large as that in the EW direction, 5.7 cm. Predominant vibrations in the NS direction were felt by many inhabitants in various regions in Kushiro City. According to the Port and Harbor Research Institute (PHRI), the Ministry of Transport of Japan,<sup>12</sup> which recorded the strong ground motion at West Port of Kushiro (see Figure 2), cyclic mobility of the sand deposits appeared in the NS-direction record, while no evidence of such phenomenon was found in the EW direction. Therefore, it is concluded that major earthquake damages were originated from the motion in the NS direction. Figures 7 and 8 illustrate the main part of the time histories of horizontal acceleration recorded by the said Meteorological Observatory<sup>13</sup> and their Fourier amplitude spectra.

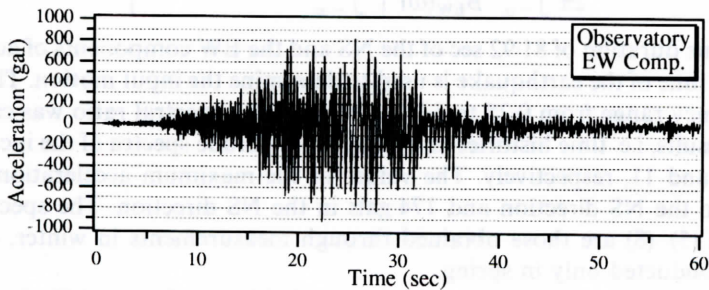
Based on the hypothesis that the spectral ratio is identical with a half of the amplification factor from diluvial bed rock to ground surface, the incident wave motion during the earthquake can be obtained. Letting  $\ddot{a}_{NS}(t)$  and  $\ddot{a}_{EW}(t)$  be the NS and the EW components of acceleration recorded at the observatory, respectively, and letting  $B_{NS}(\omega)$  and  $B_{EW}(\omega)$  be the spectral ratios of microtremor measured at the observatory in the NS and the EW directions, respectively, Fourier coefficients of the incident wave inputted at the boundary of diluvial and alluvial deposits can be given by

$$Y_{NS}(\omega) = \frac{1}{2 B_{NS}(\omega)} \int_{-\infty}^{+\infty} \ddot{a}_{NS}(t) e^{-i\omega t} dt \quad (3)$$

$$Y_{EW}(\omega) = \frac{1}{2 B_{EW}(\omega)} \int_{-\infty}^{+\infty} \ddot{a}_{EW}(t) e^{-i\omega t} dt \quad (4)$$



(a)



(b)

Figure 7. Time histories of strong ground motions recorded at Kushiro District Meteorological Observatory, (a) NS component, (b) EW component

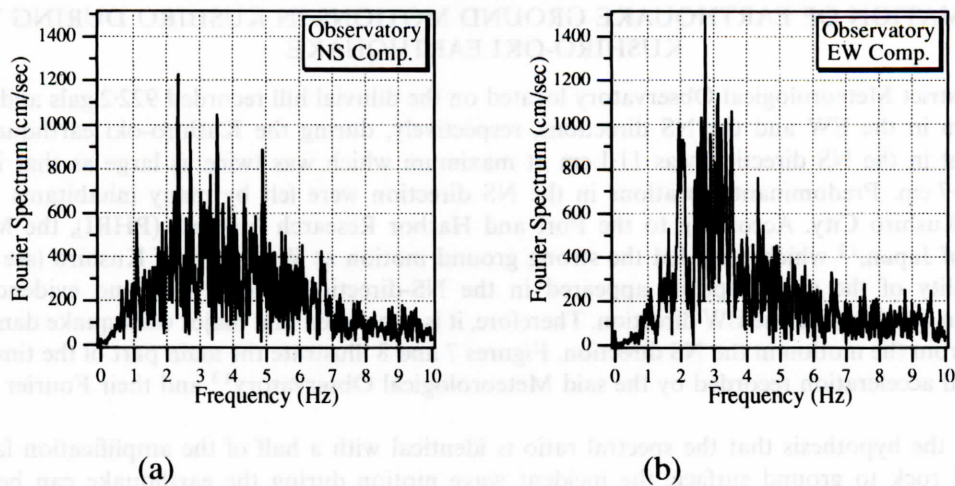


Figure 8. Fourier spectra of strong ground motions recorded at Kushiro District Meteorological Observatory, (a) NS component, (b) EW component

The spectral ratios of microtremor at the observatory used in the analyses are shown in Figure 9. Then, the earthquake ground motion during the Kushiro-oki earthquake at the microtremor measuring site,  $\alpha(t)$  in the NS direction and  $\beta(t)$  in the EW direction can be given, applying the inverse Fourier transformation as follows:

$$\alpha(t) = \frac{1}{\pi} \int_{-\infty}^{+\infty} Y_{NS}(\omega) SR_{NS}(\omega) e^{i\omega t} d\omega \quad (5)$$

$$\beta(t) = \frac{1}{\pi} \int_{-\infty}^{+\infty} Y_{EW}(\omega) SR_{EW}(\omega) e^{i\omega t} d\omega \quad (6)$$

In which,  $SR_{NS}(\omega)$  and  $SR_{EW}(\omega)$  denote spectral ratios at microtremor measuring sites in the NS and EW directions, respectively. Substituting equations (3) and (4) into equations (5) and (6), the earthquake ground motions during the Kushiro-oki earthquake at microtremor measuring sites can be obtained in the following:

$$\alpha(t) = \frac{1}{2\pi} \int_{-\infty}^{+\infty} \frac{SR_{NS}(\omega)}{B_{NS}(\omega)} \left[ \int_{-\infty}^{+\infty} \ddot{a}_{NS}(t) e^{-i\omega t} dt \right] e^{i\omega t} d\omega \quad (7)$$

$$\beta(t) = \frac{1}{2\pi} \int_{-\infty}^{+\infty} \frac{SR_{EW}(\omega)}{B_{EW}(\omega)} \left[ \int_{-\infty}^{+\infty} \ddot{a}_{EW}(t) e^{-i\omega t} dt \right] e^{i\omega t} d\omega \quad (8)$$

The main part with time duration of 81.92 sec of the NS and the EW components of acceleration recorded at the observatory at the time of the earthquake is used to determine the input motion. The analysis was carried out only in the frequency range from 0.25 to 5.0 Hz, because the spectral ratio was calculated in this range only. The analytical results, i.e. time histories and Fourier amplitude spectra of the incident wave motion are shown in Figures 10 and 11, respectively. The values of the maximum acceleration of the incident wave motion are 160 gals in the NS direction and 174 gals in the NS direction. The spectral ratios used in the analysis by equations (5)–(8) are those obtained through measurements in winter, except for sites where measurements were conducted only in spring.

As mentioned above, strong ground motions were recorded by the Port and Harbor Research Institute at West Port of Kushiro. The distance from the station of strong motion observation by PHRI to the microtremor measuring site at West Port is about 2 km, which is not a very short distance. The thickness of alluvial deposits, however, is almost the same at both sites, as shown in Figure 3. The comparison of time



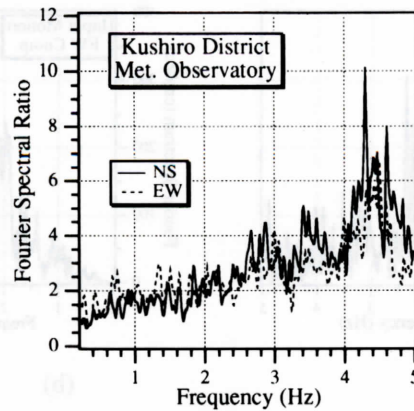
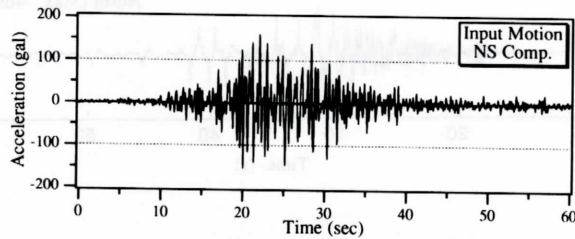
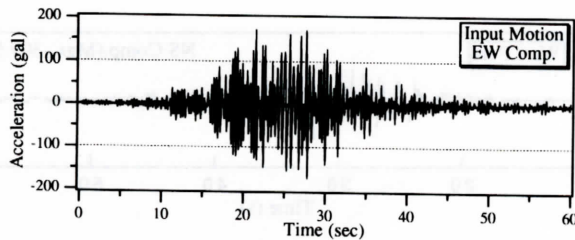


Figure 9. Special ratios at Kushiro District Meteorological Observatory,  $B_{NS}$  and  $B_{EW}$ , used in the analysis to calculate incident wave



(a)



(b)

Figure 10. Time histories of incident waves used in the analysis as input motions, (a) NS component, (b) EW component

histories in the NS direction between synthesized and recorded earthquake ground motions at West Port<sup>4</sup> is shown in Figure 12. Such comparison was not made in the EW direction, because high frequency of vibration predominates in both recorded and synthesized accelerograms. As the figure illustrates, the synthesized earthquake motion successfully approximates the recorded motion from the arrival of S-wave up to the two-thirds of the main part in the time history. In the latter one-third of the main part, the predominant period of the recorded motion becomes longer than that of the synthesized wave. In the latter half part of the recorded motion, an accelerogram with spike-like peaks can be seen. The maximum acceleration of 469 gals, which is greater than that of the synthesized motion, lies in this spike-like portion. If the spikes are removed from the accelerograms, the acceleration level is almost identical in both accelerograms in Figure 12. Thus, the method to synthesize earthquake ground motions, based on microtremor measurements proposed here, is satisfactory for estimating actual earthquake ground motions when approximating linear responses.

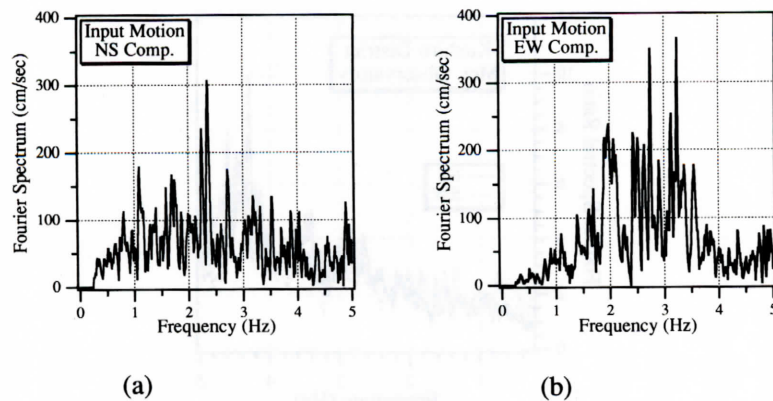


Figure 11. Fourier spectra of incident waves used in the analysis as input motion, (a) NS component, (b) ES component

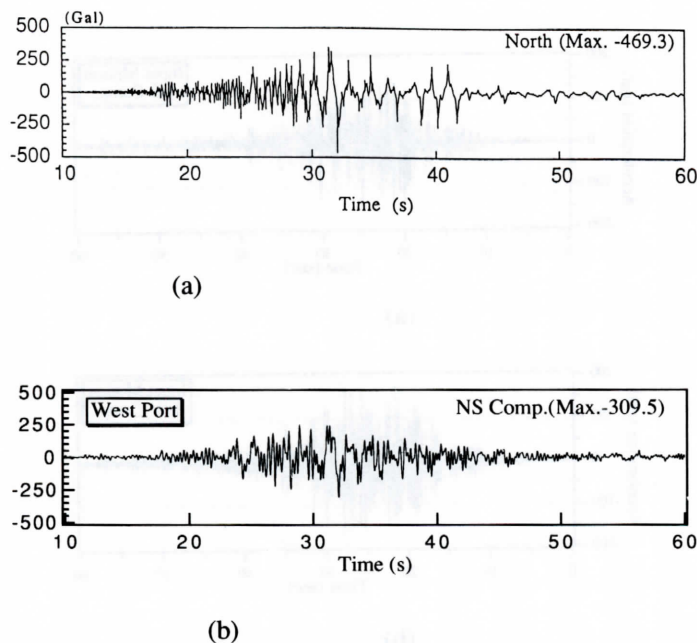


Figure 12. Comparison of the synthesized accelerogram to that recorded at West Port of Kushiro, (a) Recorded accelerogram by PHRI<sup>14</sup>, (b) Synthesized accelerogram

Time histories of synthesized earthquake ground motions at five representative sites of microtremor measurements are shown in Figure 13(a) for the NS direction and in Figure 13(b) for the EW direction. Comparing Figures 13(a) with (b), it is readily recognized that long-period vibration is predominant in the NS component, while short-period vibration is predominant in the EW component. The maximum values of acceleration in the synthesized earthquake ground motions are listed in Table II. At sites located in the Kushiro Plain, there is a tendency for the value of maximum acceleration analysed in the NS direction to be larger than that in the EW direction. At sites in the diluvial hill area, on the contrary, the value of maximum acceleration analysed in the EW direction is larger than that in the NS direction on the whole. The maximum acceleration was extremely high especially in the diluvial hill area. It should be noted, however, that these results are based on linear analyses.



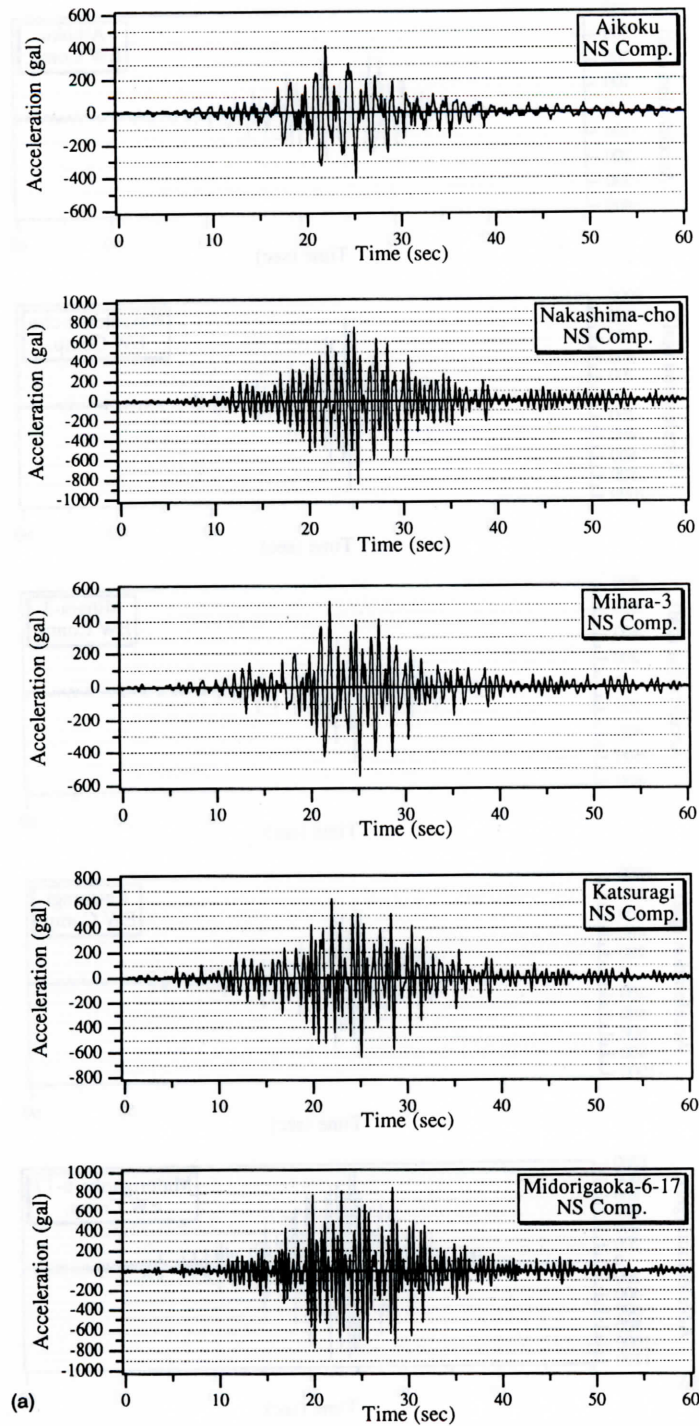


Figure 13(a). Synthesized earthquake ground motions in the NS direction at microtremor measuring sites

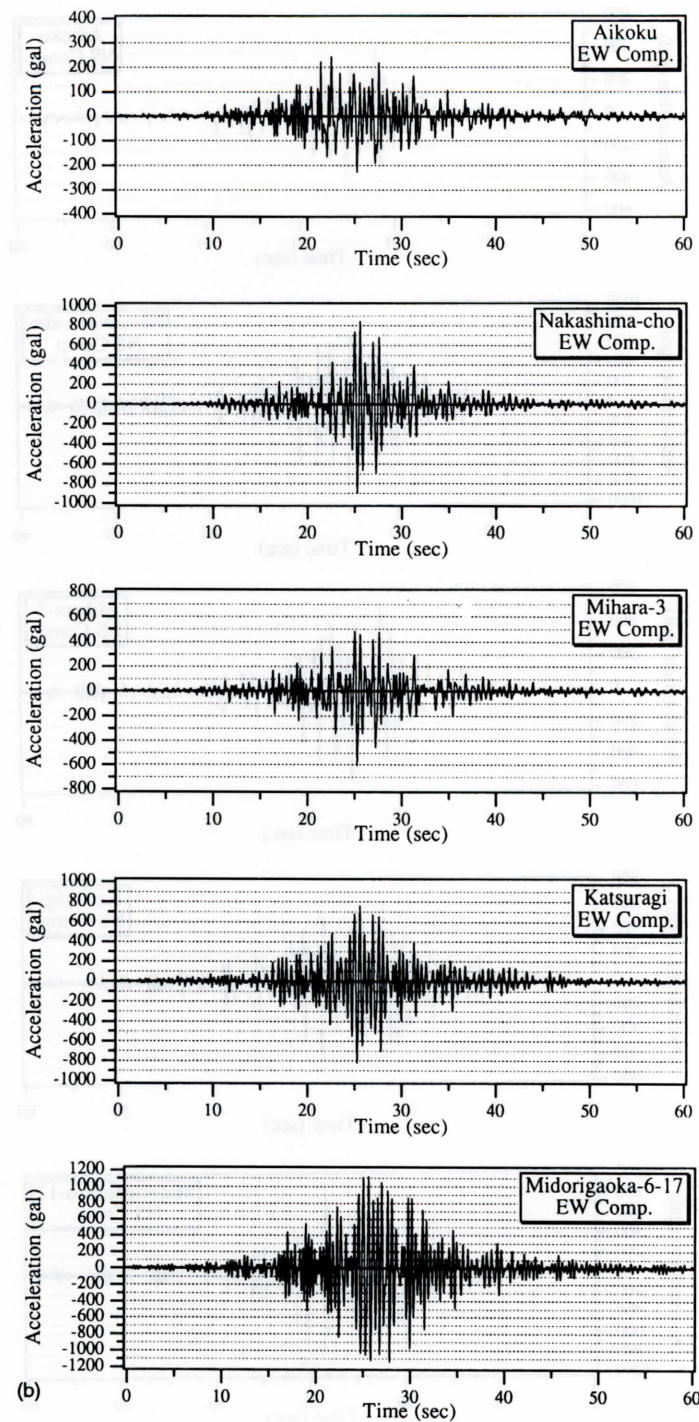


Figure 13(b). Synthesized earthquake ground motions in the EW direction at microtremor measuring sites



Table II. Values of maximum acceleration of synthesized earthquake ground motions obtained at microtremor measuring sites

Location of measurement	Maximum acceleration (gal)	
	NS comp.	EW comp.
West Port	- 309.5	437.7
Shin Fuji-cho	635.4	299.9
Tottori-ohdohri	- 657.8	234.0
Tottori-kita	- 388.3	- 291.3
Showa-cho	590.5	- 359.7
Toyokawa-cho	559.3	301.4
Aikoku	412.4	239.7
Nakashima-cho	- 848.5	- 894.0
Ashino	723.5	593.9
Mihara-3	- 544.6	- 606.1
Mihara-5	- 626.0	- 778.6
Katsuragi	- 637.1	- 820.7
Shinkai	- 570.4	- 488.1
Musa	- 1168.1	1506.2
Zaimoku-cho	- 600.7	847.3
Midorikaoka-2	1126.4	- 1152.0
Midorigaoka-6-5	1202.7	- 1617.6
Midorigaoka-6-17	845.4	- 1139.1
Midorigaoka-5	662.3	905.1

## RELATIONSHIP BETWEEN SYNTHESIZED EARTHQUAKE GROUND MOTIONS AND DAMAGES DUE TO THE KUSHIRO-OKI EARTHQUAKE

In this section, the relationship between synthesized earthquake ground motions and major damages due to the Kushiro-oki earthquake of 15 January 1993 is discussed. Figure 14 shows the earthquake damage at West Port of Kushiro, a typical damage at port and harbour facilities in Kushiro. Liquefaction occurred in the backfill of the quay wall and cracks extending parallel to the quay wall were observed. Both recorded and synthesized earthquake ground motions in the NS direction at West Port of Kushiro show cyclic behaviour with the predominant period, having a large acceleration which is considered to be sufficient for liquefying sand.

Figure 15 shows the damage due to subsidence at Mihara-3. At almost every place in the fill over marsh area, more or less significant subsidence can be observed; 30 cm of settlement at maximum was observed at Mihara-3. At Showa-cho, tilting of a few houses due to uneven subsidence of ground was observed in May, though no tilting could be found in March. This phenomenon can be explained by gradual melting down of frozen soil under the foundation of the houses. In the Miyagiken-oki earthquake of 1978, damages of industrial facilities caused by large subsidence of a peat layer occurred in Sendai City. The thickness of the peat layer in Kushiro ranges from 1 to 4 m as shown in Figure 4. The compressive coefficient  $C_c$  of peat is generally between 3.5 and 4.0 and natural water content of peat exceeds 500 per cent. Suzuki<sup>15</sup> conducted dynamic simple shear tests on the Sendai peat and concluded that the subsidence could be estimated by this parabolic equation:

$$d_p = H_p \varepsilon_a = \frac{H_p a \frac{\Delta u}{\sigma'_c}}{1 - b \frac{\Delta u}{\sigma'_c}} \quad (9)$$

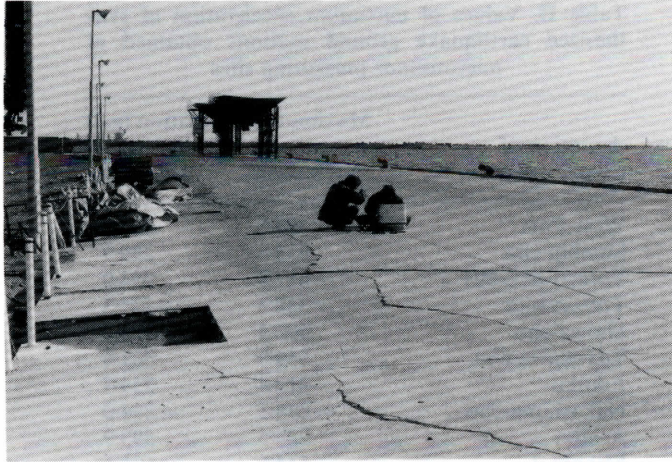


Figure 14. West Port of Kushiro. Back fill materials behind the quay wall liquified at West Port of Kushiro, which led to the wide-spread cracks on a concrete pavement



Figure 15. Mihara-3. Dissipation of pore-water pressure built up in the peat layer subjected to the Kushiro earthquake might cause large subsidence measuring over 20 cm at Mihara-3

in which  $d_p$ ,  $H_p$  and  $\varepsilon_a$  denote subsidence, thickness and axial strain (per cent) of the peat layer, respectively;  $\Delta u/\sigma'_c$  excess pore-water pressure ratio; and  $a$  and  $b$  denote constants determined experimentally depending on the soil material, respectively. As shown in Figure 13, the maximum accelerations of synthesized earthquake ground motions at Mihara-3 are 545 and 605 gals in the NS and the EW directions, respectively. The value of  $\Delta u/\sigma'_c$  may increase up to 0.6 or 0.7. Letting  $H_p$  be 3.0 m and using constants  $a$  and  $b$  equal to those of Sendai peat, i.e.  $a = 2.875$ ,  $b = 1.0$ ,  $d_p$  becomes 20.1 cm for  $\Delta u/\sigma'_c = 0.7$  and 12.9 cm for  $\Delta u/\sigma'_c = 0.6$ . Consequently, the main cause of the subsidence may be consolidation of the peat layer due to the dissipation of excess pore-water pressure.

Figure 16 shows the uplift of a manhole of sewer trunk at Katsuragi, where the maximum acceleration was estimated as 637 gals in the NS direction and 821 gals in the EW direction. The thickness of alluvial deposits there is about 40 m.



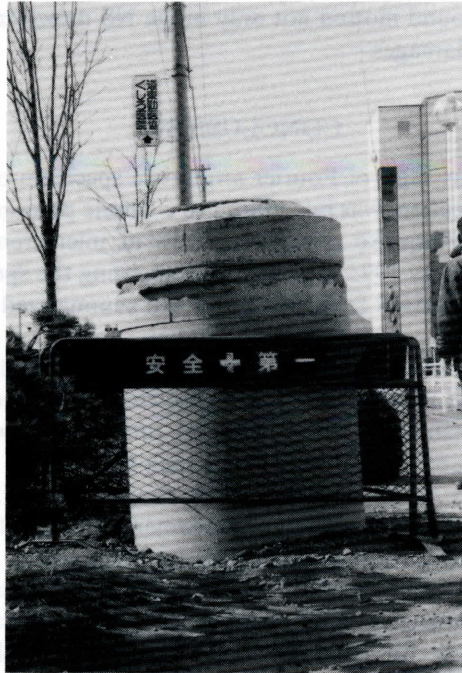


Figure 16. Katsuragi. More than 20 manholes of two sewer mains along the road were floated up due to liquefaction at Katsuragi and Kiba. 1.5 m of lift-up at maximum was observed



Figure 17. Midorigaoka-6. Large-scale slope failures took place and several houses were destructively damaged at Midorigaoka. Acceleration which reaches  $1g$  was estimated in the analyses at Midorigaoka

The slope failure that took place at Midorigaoka is shown in Figure 17. The maximum values of synthesized earthquake ground motions at four sites at Midorigaoka were surprisingly large as we see in Figure 13 and Table II. The microtremor measuring site at Midorigaoka-6-17 is located 20–30 m away from the slope failure in the figure. The maximum acceleration there is 845 gals in the NS directions and 1139 gals in the EW direction. At other sites at Midorigaoka, the maximum acceleration also exceeds  $1g$  as shown in Table II. Thus, the acceleration at Midorigaoka is considered to be sufficient to cause slope failures. In the

diluvial hill area, therefore, the ground motion not only in the NS direction but also in the EW direction is estimated to have caused severe damages.

## CONCLUSIONS

In this paper, the spectral ratio, i.e. ratio of Fourier amplitude spectrum of microtremor in the horizontal direction to that in the vertical direction, was introduced to evaluate predominant vibrations at various sites in Kushiro City. In addition, earthquake ground motions at microtremor measuring sites during the Kushiro-oki earthquake of 15 January 1993 were synthesized, using the spectral ratio equal to a half of the amplification factor. Conclusions derived from this paper are summarized as follows:

- (a) With regard to microtremors, the spectral ratio demonstrates the predominant frequency of the surface layer more clearly than the Fourier amplitude spectrum of the horizontal component does. The predominant frequency obtained from the spectral ratio agrees well with the natural frequency expected from the thickness of alluvial deposits at each site.
- (b) The predominant frequency in the Kushiro Plain ranges from 0.5 to 1.7 Hz. The spectral ratio demonstrates a clear peak at the frequency of fundamental mode of the surface layer. On the other hand, the spectral ratio in the diluvial hill area does not show a peak as clear as that in the plain does. The peak with a wide band from 2 to 4 Hz was obtained in the diluvial hill area.
- (c) There is no remarkable difference in spectral ratios between the data obtained in winter and spring. There is a tendency, however, for the spectral ratio in spring to show a little higher value in the frequency range higher than 2 Hz.
- (d) The synthesized earthquake ground motion at West Port of Kushiro simulated successfully the recorded earthquake ground motion. This demonstrates the applicability of the analytical approach proposed in this paper.
- (e) According to the synthesized earthquake ground motions for the Kushiro-oki earthquake, the earthquake ground motion in the NS direction was the main cause of earthquake damages in the Kushiro Plain, while damages in the diluvial hill area were attributable to earthquake ground motions both in the NS and EW directions. At Midorigaoka, acceleration exceeding 1  $g$  was estimated to have taken place.

The spectral ratio used in this paper may be modified in consideration of the source mechanism and the travelling process of microtremor, in the case of more precise evaluation of predominant vibrations of surface deposits. Furthermore, it should be noted that the microtremor-spectral-ratio approach discussed here to synthesize earthquake ground motions, deals with the linear response problem only. Therefore, the extension of this strategy, by means of the equivalent linear technique for example, is required to cover non-linear response problems. These two items are subjects to our future research.

## REFERENCES

1. T. Suzuki, 'Lessons learned from the 15 January 1993 Kushiro-oki earthquake', in *Proc. 3rd int. forum on seismic zonation*, Memphis, 1993, pp. 37–40.
2. Y. Nakamura, 'On a method of dynamic characteristics estimation for railway embankments using microtremor' *Railway Technical Research Institute (RTRI) Report*, Vol. 2, No. 7, 1988, pp. 34–43.
3. Y. Nakamura and T. Takizawa, 'The surface layer thickness and the shearing wave velocity of basement and surface estimated by microtremor measurement', *RTRI Report*, Vol. 4, No. 9, 1990, pp. 29–35 (in Japanese).
4. Y. Nakamura, T. Ohmachi and T. Toshinawa, 'Relationship between characteristics of earthquake ground motions estimated from microtremor measurements and earthquake damage in Loma Prieta earthquake', *Proc. JSCE*, Vol. 424, No. 3–14, 1990, pp. 37–51 (in Japanese).
5. T. Ohmachi and Y. Nakamura, 'Local site effects detected by microtremor measurements on the damage due to the 1990 Philippine earthquake', in *Proc. 10WCEE*, Madrid, 2, pp. 997–1002 (1992).
6. Y. Okazaki, S. Sato and H. Nagahara, 'Explanatory text of the geological map of Japan on a scale of 1/50 000—Otanoshige (Kushiro-35)—', Geological Survey of Japan, 1966.
7. L. Lu, F. Yamazaki and T. Katayama, 'Soil amplification based on seismometer array and microtremor observations in Chiba, Japan', *Earthquake eng. struct. dyn.* 21, 95–108 (1992).



8. Y. Nakamura, 'A method for dynamic estimation of surface layers using microtremor on the surface', *RTRI Report*, Vol. 2, No. 4, 1988, pp. 18–27 (in Japanese).
9. C. Tamura, Y. Hinata and T. Suzuki, 'Earthquake observation and response analysis of a shield tunnel', in *Proc. 9WCEE*, Tokyo and Kyoto, **6**, 563–568 (1988).
10. T. Suzuki and K. Unami, 'The extended quasi-three-dimensional ground model for irregularly bounded surface ground', *Struct. eng. earthquake eng. JSCE* **9** (1), 33s–43s (1992).
11. Kushiro District Meteorological Observatory, 'Quick report on the strong motion record observed at Kushiro District Meteorological Observatory', 1993.
12. T. Kanbe, 'Damage of port, harbor and airport facility due to the Kushiro-oki earthquake of 15 January 1993', Quick Report on the Kushiro-oki Earthquake by Earthquake Eng. Committee, JSCE, 1993, pp. 27–30 (in Japanese).
13. The Meteorological Agency of Japan, 'Earthquake strong motion data set during the Kushiro-oki earthquake of 15 January 1993', 1993.
14. Y. Matsunaga, S. Iai and T. Kameoka, 'The effect of liquefaction prevention works for quay walls during the Kushiro-oki earthquake of 15 January 1993', *Proc. the 22nd earthq. eng. symp.*, JSCE, 1993, pp. 399–402 (in Japanese).
15. T. Suzuki, 'Settlement of saturated clays under dynamic stress history', *J. Japan soc. eng. geology* **25–3**, 21–31 (1984) (in Japanese).